Eur Biophys J (2007) 36:771–778
DOI 10.1007/s00249-007-0152-4

ORIGINAL PAPER

A novel technique to study pore-forming peptides in a natural membrane

Natascia Vedovato · Giorgio Rispoli

Received: 18 December 2006 / Revised: 10 February 2007 / Accepted: 26 February 2007 / Published online: 16 March 2007

Abstract The biophysical characteristics and the pore formation dynamics of synthetic or naturally occurring peptides forming membrane-spanning channels were investigated by using isolated photoreceptor rod outer segments (OS) recorded in whole-cell configuration. Once blocking the two OS endogenous conductances (the cGMP channels by light and the Na^+:Ca^{2+},K^+ exchanger by removing one of the transported ion species from both sides of the membrane, i.e. K^+, Na^+ or Ca^{2+}), the OS membrane resistance (R_m) was typically larger than 1 GΩ in the presence of 1 mM external Ca^{2+}. Therefore, any exogenous current could be studied down to the single channel level. The peptides were applied to (and removed from) the extracellular OS side in ∼50 ms with a computer-controlled microperfusion system, in which every perfusion parameter, as the rate of solution flow, the temporal sequence of solution changes or the number of automatic, self-washing cycles were controlled by a user-friendly interface. This technique was then used to determine the biophysical properties and the pore formation dynamics of antibiotic peptaibols, as the native alamethicin mixture, the synthesized major component of the neutral fraction (F50/5) of alamethicin, and the synthetic trichogin GA IV.

N. Vedovato · G. Rispoli (✉)
CNISM, Dipartimento di Biologia ed Evoluzione,
Sezione di Fisiologia e Biofisica and Centro di
Neuroscienze, Università di Ferrara, via Borsari 46,
44100 Ferrara, Italy
e-mail: rsg@unife.it

Present Address:
N. Vedovato
Laboratory of Cardiac/Membrane Physiology,
The Rockefeller University, 1230 York Avenue,
New York, NY 10021, USA

Keywords Ion channels · Patch clamp · Peptide antibiotics · Photoreceptors · Pore-forming toxins · Single-channel recording

Abbreviation

OS	Photoreceptor rod outer segment
V_h	Holding potential

Introduction

Proteins and peptides that form membrane-spanning pores and channels comprise a diverse class of molecules. These ranges from short peptides, that are unregulated and non-selective, to large proteins that are highly regulated and exhibit exquisite selectivity for particular ions.

Short peptides have a strong anti-microbial activity, since pore formation in the membrane of bacteria leads to lyses and death, therefore physicochemical studies of peptide–lipid interactions provide attractive approaches for drug design (Duclohier 2002). A large amount of studies has been carried out in the last 30 years on peptaibols, a group of naturally occurring short peptides produced by fungi of the genus *Trichoderma*, possessing anti-microbial activity. They form helices characterised by an N-terminal acyl group, a C-terminal 1,2-aminoalcohol and a high content of the non-proteinogenic α-amino acid Aib (α-amino-isobutyric acid). Long peptaibols, such as alamethicin, are supposed to pack together in parallel around a central ion-permeable pore once in the plasma membrane ("helix bundle" or "barrel stave" model; Boheim 1974; Eisenberg et al. 1973), resembling the structural motif of the pore region of basically all cellular ion channels.

Enhanced membrane permeability is typically observed also during infection of susceptible cells by most animal

viruses (Carrasco 1995). The viral genes responsible for these changes are classified as viroporins, coding small (<100 residues) membrane proteins forming amphipathic alfa helices. The insertion of these proteins into membranes followed by their oligomerisation creates a hydrophilic pore. There are currently about a dozen proteins that qualify as viroporins, as HIV-1, M2 protein from influenza virus A and B and protein 2B from poliovirus (Gonzales and Carrasco 2003), all considered good candidates to explore one of the major feature of viral infection.

Bacterial and viral peptides would also provide a simple model system to understand the structure–function relationships in ion channels, the development of ion channel activity and selectivity, the possibility to manipulate channel activity with small molecule modulators, and the molecular basis of peptide/protein oligomerisation in lipid membranes. The diversity of regulation and selectivity, together with recent advances in protein "re-engineering" technology, provide also a strong framework on which to build custom made molecules with wide-ranging biotechnological applications. Numerous pore-forming peptides (native or re-engineered) are currently under development to create targeted and regulable cell-killing agents, that could have antimicrobial and anti-tumorigenic activity (Oh et al. 2000; Toniolo et al. 2001). Peptide engineering may provide also a pharmacological approach to cure channelopaties; in this case a synthetic channel could be inserted in cells expressing an aberrant ion channel. Encouraging results have already been obtained in human epithelia of the cystic fibrosis patients with a defective chloride channel (Wallace et al. 2000).

Despite the very large number of studies on transmembrane proteins carried out in the last twenty years, the structural bases of pore formation and assembly have been determined experimentally for only a few of the proteins and protein complexes (Heuck and Johnson 2002). Moreover, although interactions between proteins and lipids lie at the heart of virtually all membrane processes, they are still poorly understood at the molecular level (Killian and Nyholm 2006). To understand how this interaction induce optimal peptide orientation and mutual structural changes to produce a raise in membrane conductance (Chen et al. 2001; Saint et al. 2002), several studies have been carried out on peptides inserted in different artificial membranes, using non-physiological voltages and ionic gradients that could affect the peptide itself, or even the membrane in which they were inserted (Bockmann et al. 2003). Moreover, to our knowledge, no studies addressed directly the kinetics with which peptides assemble and disassemble to form a functioning pore in a cell membrane.

In this paper, the strategy employed to study peptides under strict physiological conditions consisted in inserting the peptides in cell plasma membranes where all the endogenous current sources were blocked. By using whole-cell patch-clamp recordings, peptides insertion would be then detected by the manifestation of an exogenous current. It has been found that the isolated rod outer segment (OS; Rispoli et al. 1993) was particularly suitable to carry on the above studies, because it was possible to block easily all the endogenous currents without using any drug (such as TTX, TEA, dihydropyridine, etc.), that could obstruct the peptide pores (or interfere with the pore formation) as well. In particular, the extracellular solution could be changed in ~50 ms using a computer controlled microperfusion system developed in collaboration with an industrial partner (De Angelis s.r.l., Genoa, Italy; Fig. 1). This system allowed rapid application and removal of ions, drugs and peptides on the cells with a controlled timing, so that the ion channel characteristics (as its selectivity, blockade and gating; Hille 2001) and the dynamics of pore formation could be precisely assessed.

Materials and methods

Animals and preparation

Rana esculenta frogs were kept in filtered, running tap water in small tanks at room temperature (20–23°C), fed two-three times a week with honey worms and maintained in a natural light-dark cycle. Animal experiments and care were performed in compliance with the Declaration of Helsinki guidelines and with the approval of a local ethical committee.

Before dissection, the animals were dark adapted (≈4 h), anaesthetised by immersion in a tricaine methane sulphonate solution (1 g/l in water) and then decapitated. Both eyes were removed from the head and hemisected. The back half of the eyeball was cut into four pieces that were stored in oxygenated Ringer solution on ice and used when needed. The retina was "peeled" from an eyecup piece and was gently triturated in ~5 µl of Ringer, using a fire-polished Pasteur pipette to obtain the OS. All these manipulations were made in the dark using infrared illumination and an infrared viewer (Find-R-Scope, FJW Optical Systems, Palatine, IL, USA).

Solutions and peptides

Cells were bathed in Ringer's solution having the following composition (in mM): 115 NaCl, 3 KCl, 10 HEPES free acid (N-(2-hydroxyethyl)piperazine-N′-(2ethanesulfonic acid)), 0.6 $MgCl_2$, 0.6 $MgSO_4$, 1.5 $CaCl_2$, 10 glucose (osmolality 260 mOsm/Kg, buffered to pH 7.6). Peptides were applied and removed in ~50 ms by switching forth and back the OS from a stream of control perfusion solution

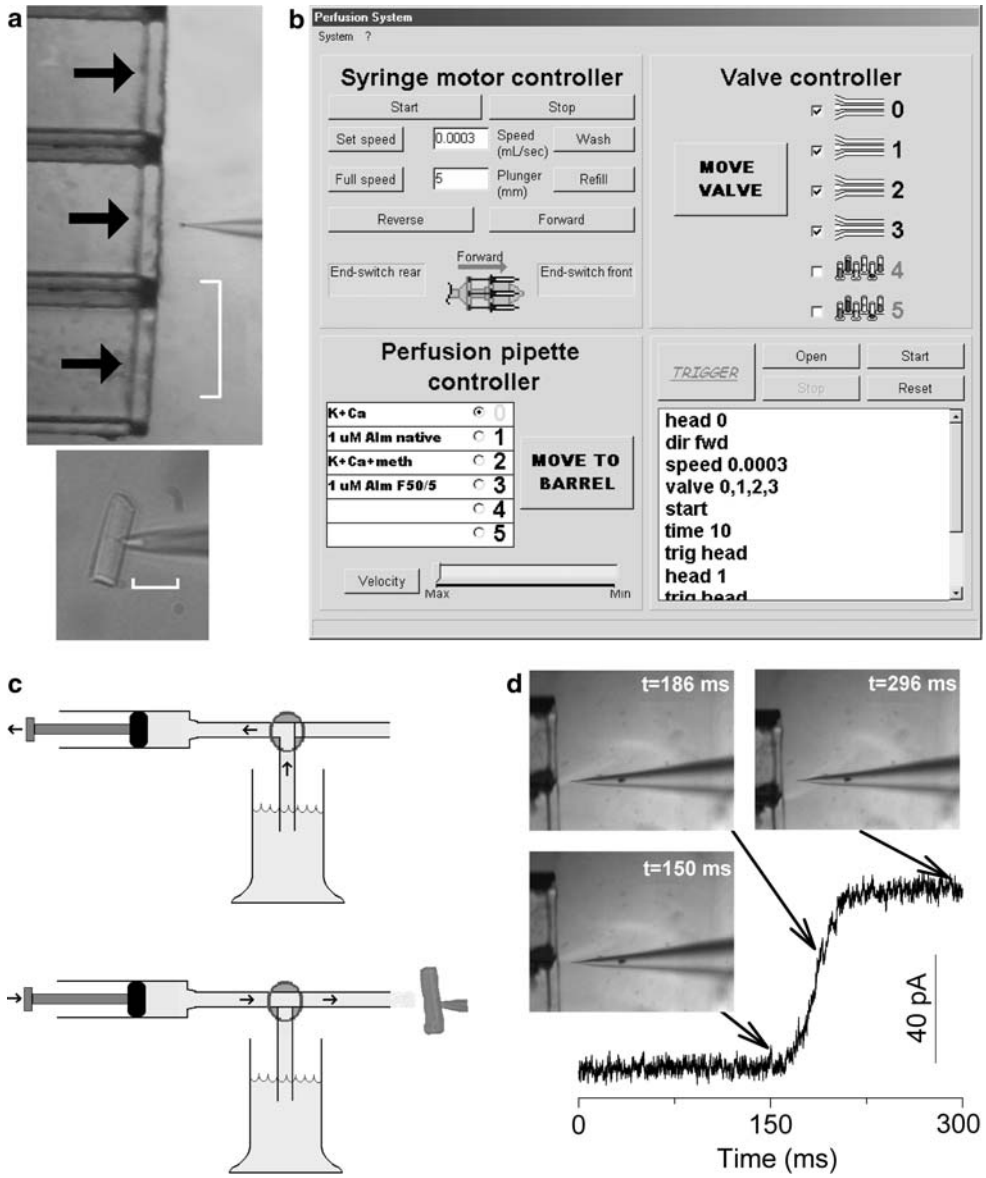

Fig. 1 The technique employed to investigate the permeabilisation properties of the peptides inserted in a natural membrane. **a** *Upper panel*, isolated rod outer segment (OS) recorded in whole-cell mode aligned in front of the multibarreled perfusion pipette (scale bar is 500 μm, *horizontal black arrows* denote perfusion flows); *lower panel*, the same OS at higher magnification (scale bar is 20 μm). **b** User interface of the perfusion apparatus described in Methods. **c** Scheme of one perfusion line (composed by a syringe, a three-way valve, a cylinder and one perfusion pipette barrel) and perfusion flow during syringe refilling (*upper panel*) and during perfusion of an OS recorded in whole-cell (*lower panel*); drawing not in scale. **d** *Trace* shows the current jump upon switching an open pipette (9 MΩ, $V_h = 0$ mV) from 65 mM choline + 65 mM K^+ + 1 mM Ca^{2+} to a solution identical to the patch pipette solution (130 mM K^+ + 1 mM Ca^{2+}). The two solutions had a 0.6 mV junction potential, producing a current jump of 70 pA, lasting ∼50 ms, that had the same kinetics of the solution change. The kinetics of the solution change is also shown by the three still frames (650 × 494 pixels at 12 bits grey-scale resolution), extracted from a 30 frame/s movie synchronised with the voltage-clamp recording. The boundary separating the two solution streams was clearly visible, allowing a precise electrical and visual correlation of the solution change dynamics

(composition (in mM): 130 K^+ or 130 Na^+, 1 Ca^{2+} and 10 HEPES; osmolality 260 mOsm/Kg, buffered to pH 7.6 with KOH or NaOH) to a stream containing the peptide (dissolved in the same perfusion solution). Patch pipettes were filled with the same perfusion solution in order to drive the current just with the holding voltage (V_h), that was typically −20 mV. Peptides were dissolved in methanol to get a 1 or 0.1 mM stock solution. An aliquot of this stock was dissolved in the perfusion solution to obtain the final concentration (usually 0.1, 0.25, 1 or 6 μM), and used within 30 min. Control experiments proved that the maximal methanol contamination of the perfusion solution (∼10 μl/ml) did not cause any non-specific membrane permeabilisation. The perfusion solution was removed by a peristaltic

pump (OEM 400VDL/VM3, Watson Marlow, Wilmington, MA, USA).

The native alamethicin mixture and all the other chemicals were purchased from Sigma-Aldrich (St. Louis, MO, USA). The primary structure of synthesized alamethicin F50/5 was: Ac-Aib-Pro-Aib-Ala-Aib-Ala-Gln-Aib-Val-Aib-Gly-Leu-Aib-Pro-Val-Aib-Aib-Gln-Gln-Phol (where Aib is α-aminoisobutyric acid, Ac is acetyl, and Phol is phenylalaninol); the primary structure of natural trichogin GA IV (Peggion et al. 2003; Auvin-Guette et al. 1992) was: n-Oct-Aib-Gly-Leu-Aib-Gly-Gly-Leu-Aib-Gly-Ile-Lol (n-Oct is n-octanoyl and Lol is leucinol). The synthesized version that was used in the following had a leucine methyl ester at the C-terminus replacing Lol. Peptide synthesis was carried out in solution using the segment condensation approach (Peggion et al. 2004).

Patch-clamp recordings and data analysis

In dim room lights, a fluid drop (500 µl) of the triturated retina was transferred to the recording chamber on the microscope stage (TE 300, Nikon, Tokyo, Japan), fitted with an Eppendorf micromanipulator (model 5171, Eppendorf, Hamburg, Germany). The OS were illuminated with an ultrabright infrared LED (900 nm) and viewed in a window of AquaCosmos software package (version 2.5.3.0; Hamamatsu Photonics, Tokyo, Japan) controlling via a PCI board (PCDIG, Dalsa, Waterloo, Ontario, Canada) a fast digital camera (C6790-81, Hamamatsu Photonics) coupled to the microscope.

Electrical recordings were carried out using the patch-clamp recording technique in the "whole-cell" configuration, under visual control at room temperature (20–23°C), employing Axopatch 200B (Axon Instruments, Union City, CA, USA). Pipettes were pulled in the conventional manner from 50 µl glass capillaries (Drummond, Broomall, PA, USA), and fire-polished to a pipette resistance of ≈5 MΩ.

Seal resistance (range: 5–50 GΩ), access resistance (19.2 ± 1.1 MΩ), membrane resistance (R_m; 1.4 ± 0.2 GΩ) and cell capacitance (11.6 ± 0.5 pF) were determined using -10 mV voltage pulses (40 OS averaged). Recordings were filtered at 2 kHz via an eight-pole Butterworth filter (VBF/8 Kemo, Beckenham, UK), sampled on-line at 10 kHz by a Digidata 1322A connected to the SCSI port of a Pentium computer running the pClamp software package (version 9.0; Molecular Devices, Sunnyvale, CA, USA), and stored on disk. Data were further low-pass filtered off-line at 200 Hz using a Gaussian filter and analysed using Clampfit (included in the pClamp package). The parameters characterising the membrane permeabilisation induced by the peptides were measured on the traces smoothed using the "running average" routine of SigmaPlot or by low pass filtering the traces using a Gaussian filter at 20 Hz, to avoid errors produced by the noise. Figures and statistics were performed using SigmaPlot (version 8.0; Jandel Scientific, San Rafael, CA, USA); results are given as means ± SEM.

Fast perfusion system

After obtaining the whole cell recording, the OS (Fig. 1a, upper panel) was aligned in front of a multi-barreled perfusion pipette of a fast microperfusion system (Fig. 1a, lower panel). The perfusion pipette was moved on a horizontal plane with a precision step motor, controlled by a user-friendly interface (Fig. 1b, perfusion pipette controller panel) running in a host computer, connected to the microperfusion system via the serial port. The perfusion pipette was constituted of up to six barrels (500 µm of side; three barrels of a four barreled pipette are visible in Fig. 1a, upper panel) made with precision, square glass capillaries glued together. Peptides were applied and removed in ~50 ms (see below) by moving the perfusion pipette so that to switch the whole-cell recorded OS back and forth from a stream of control perfusion solution (usually containing 130 mM of a monovalent cation and 1 mM Ca^{2+}; see Results) to a stream containing the peptide (dissolved in the same perfusion solution). This strategy allowed to assess the dynamics of the pore formation and the possible reversibility of the process. This system could be also used to perfuse the OS with solutions of different ionic composition or containing a specific drug, so that to study, besides the current-to-voltage characteristics, the ion selectivity and blockade of the pore as well. To this aim, all perfusion solutions contained the peptide under study at the same concentration, so that to compare the effects of the test solutions at a constant membrane permeabilisation.

The solutions flowing in the perfusion pipette were fed by means of precision syringes (Hamilton, Reno, NV, USA), whose piston was moved by a DC motor controlled via the computer interface (Syringe motor controller panel, Fig. 1b). The typical perfusion speed was 15 µl/min, therefore minimal amounts of peptide solution (<500 µl) were required to perform peptide applications lasting more than half an hour. The fine regulation of the perfusion flow speed and of the velocity of perfusion pipette horizontal movements (controlled by the Velocity button in the Perfusion pipette controller panel) allowed to perform fast solution changes on practically any isolated cell type, or even on small cell aggregates, without any significant change of the seal resistance. This system has been successfully tested on isolated inner ear hair cells, HEK293 and COS cultured cells, enzymatically dissociated retinal cells, and on enzymatically dissociated rat cardiomyocytes. Depending upon the position of the six three-way solenoid valves (Fig. 1c; all tubing and valve components in contact with the solutions were made in teflon), each one independently

controlled by the valve controller panel (Fig. 1b), the solution contained in each syringe could be sent to the perfusion pipette (symbolised by the perfusion pipette in the valve controller panel; Fig. 1b) or redirected to one of the six reservoirs (in which each solution was made, symbolised by a group of cylinders in the valve controller panel). This allowed to save the solutions that were not used, or to avoid that, upon switching between two non adjacent barrels, the OS was transiently exposed to a third undesired solution. Once emptied, the syringes could be refilled from the cylinders by clicking on the refill button (in the syringe motor controller panel, Fig. 1b). This command moved the six three-way valves in the cylinder position and backed up the DC motor at full speed until the syringes were filled: the motor was then stopped by an end-position switch (a second end-position switch stopped the motor when syringes were emptied; the status of the switches was signaled by the end switch rear and the end switch front indicators in the syringe motor controller panel). At the end of the experiment, all the perfusion lines could be washed by dipping all the tubes previously dipped in the cylinders, into a container filled with distilled water (or other washing solution, as methanol, ethanol, DMSO, and so on), and clicking the wash button. This command activated the valves and moved the motor back and forth at full speed, so that the syringes were emptied through the perfusion pipette and refilled with the wash solution a number of times set by the user in a sub-window opened by the wash button (not shown).

The timing and sequence of the solution changes (i.e. the direction, speed and travel of the perfusion pipette step motor), the syringe motor speed, start, stop and direction, and each valve position could be also automatically controlled by simple instructions, entered as a text code (shown in the white window of Fig. 1b). A set of instructions of arbitrary length could be executed in sequence by clicking on the Trigger button; each instruction could be executed after a delay set by the instruction time, that would therefore set the sequence timing. Every instruction could be also executed after receiving a trigger pulse from an external device, allowing, for example, the synchronization of the solution changes with the pClamp voltage protocols (as in the experiments shown in Fig. 3 and Fig. 4a) or with an imaging system (as in the experiments of Fig. 1d). It was also possible to send out a trigger pulse, after executing a set of instruction of arbitrary length, to synchronize other devices.

The temporal lag between the time in which the command (internal or triggered by an external device) moving the perfusion pipette was imparted, and the time in which the solution change effectively occurred, as well as the speed of the solution change, were occasionally measured (since they were very reproducible) as illustrated in Fig. 1d. At the end of experiment, the cell was blown off the patch pipette with a positive pressure pulse, and the odd perfusion lines were filled with a solution having 50% choline chloride and 50% KCl, while the even perfusion lines were filled with the patch pipette solution. The choline chloride had a different index of refraction in respect to all the patch pipette solution used, therefore the boundary separating two adjacent streams was clearly visible (see the three still frames of Fig. 1d). Since a junction potential was also developed between the two solutions, upon repeating the solution changes previously performed with the OS, a current jump was recorded by the open pipette (voltage-clamped at 0 mV) that had the same kinetics of the solution change (Fig. 1d). By comparing the electrical and the imaging recordings, it results that the solution change was completed within the 50 ms necessary to the OS to cross the boundary separating two adjacent streams.

Results and discussion

To study the biophysical properties of a pore-forming peptide inserted in a natural membrane, it was planned to extracellularly perfuse the peptides on a cell where all the endogenous sources of membrane current could be readily blocked. The photoreceptor rod outer segments (OS) mechanically isolated from *R. esculenta* frogs have been found particularly suitable to carry on this study, because of their large size (Fig. 1a, lower panel) and for the commercial availability and low cost of this frog species. The frog OS, as the OS of all vertebrates, possesses just two endogenous conductances: the light sensitive channels and the Na^+:Ca^{2+},K^+ exchanger (reviewed in Rispoli 1998; Moriondo and Rispoli 2003). If the OS is illuminated, the light sensitive channels close; moreover, the exchanger can be blocked if just one of the ion species transported by it (i.e. Na^+, Ca^{2+} or K^+) is removed from both sides of the membrane (Rispoli et al. 1995). The exchanger current can be also reduced to a negligible amplitude by minimizing the electrochemical gradients of the transported ions. Moreover, the OS contains just the enzymes necessary to perform phototransduction, thus minimizing any possible interactions of peptides with OS endogenous cytoplasmic proteins.

To simplify the interpretation of the experiments, patch pipettes were filled with the same perfusion solution (that typically contained 130 mM of a monovalent cation) to ensure the current was only driven by V_h (usually set to −20 mV). Under these conditions and in the absence of the peptide, the OS R_m was usually larger than 1 GΩ under room lights (that will close all the light-regulated channels), exhibiting a linear (ohmic) current-to-voltage characteristics (similar to the one illustrated in Fig. 2a). This high R_m

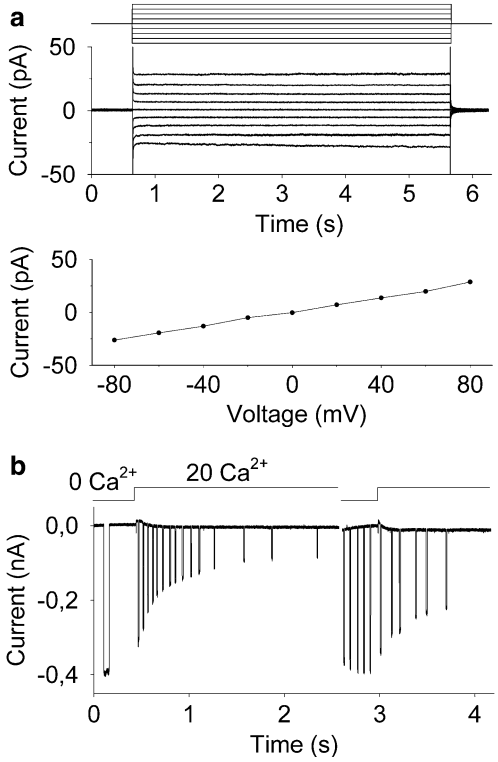

Fig. 2 Electrical properties of OS. **a** *Upper panel*: average whole-cell current recorded from a representative OS under room lights (pipette and external solution: 130 mM K^+ + 1 mM Ca^{2+}), subjected to 5 s voltage steps from −80 mV to +80 mV in 10 mV increments (*top traces*) starting from V_h = 0 mV and repeated 10 times; *lower panel*, the average current recorded for each voltage step shown in the *upper panel* is plotted against the voltage step (the resulting current to voltage characteristics is linear, giving $R_m \sim 3$ GΩ). **b** Extracellular Ca^{2+} dependence of R_m. An OS dialysed with 130 mM K^+ + 1 mM Ca^{2+} and kept for ∼20 min in a 130 mM K^+ + 0 Ca^{2+} solution, was switched to a 100 mM K^+ +20 mM Ca^{2+} perfusion solution while continuously measuring R_m with repetitive −20 mV voltage pulses. Note that ∼2 s of high external Ca^{2+} application was enough to rise R_m of about five-fold (from ∼50 to ∼250 MΩ) and that R_m recovered its previous low value upon removing external Ca^{2+}

value allowed current recordings with a resolution of 1 pA in a bandwidth of at least 1 kHz; however, low values of R_m (<100 MΩ) were often measured in the absence of external Ca^{2+}. R_m was unaffected upon applying K^+ channel blockers (as 10 mM TEA) to the 0 Ca^{2+} solution, but it was augmented by reintegrating external Ca^{2+} (Fig. 2b). This indicates that the low R_m originated by a reversible membrane leakage produced by the lack of Ca^{2+}. Since the OS does not possess Ca-activated proteases (that are instead present in the inner segment), it was possible the long-lasting dialysis of the OS (>1 hr) with high Ca^{2+} solutions. Therefore, in all experiments 1 mM Ca^{2+} was incorporated in the external solution, to preserve the membrane integrity, and in the internal solution as well, to ensure the current was driven only by V_h.

The dynamics of the pore formation was tested by means of the following protocol (Figs. 3 and 4). With the isolated OS continuously held to V_h, R_m was measured before peptide perfusion; the peptide was then quickly applied (∼50 ms) using the fast perfusion system. Once the current had stabilised, the OS were finally returned to the control solution (without the peptide) to assess a possible recovery of the current, and R_m was again measured.

This protocol was applied first using the native, commercially available alamethicin mixture, consisting of ∼85% of the F30 components and of ∼12% of the F50 components (see Sigma-Aldrich on-line catalogue for details). The peptide application at a concentration of 1 μM produced a large OS membrane permeabilization, after a delay of 1.9 ± 0.2 s (n = 3), as shown by the exponential increase of current (activation time constant of 7.6 ± 2.4 s, n = 3) to a steady state value (300 ± 60 pA, n = 3; Fig. 3). The permeabilisation was fully reversible: the current returned to the zero level, and R_m recovered his previous (high) value, once the peptide was removed from the external solution (Fig. 3). The current recovery was again exponential, begun without any delay with respect to the peptide removal time, and its deactivation time constant was much faster than the activation one (1.7 ± 0.5 s, n = 3). It can be concluded that the native alamethicin mixture applied to a natural membrane at a concentration as low as 1 μM requires about a couple

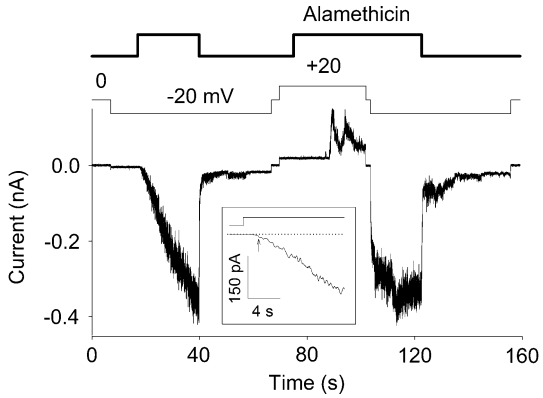

Fig. 3 Kinetics of OS membrane permeabilisation induced by 1 μM concentration of the native, commercially available, alamethicin mixture. Traces show, from top to bottom, the timing of the peptide application and withdrawal, the V_h timing, and the voltage-clamp, whole-cell current recordings from the OS. The membrane resistance was 4.7 GΩ before peptide application, it fell to ∼60 MΩ at the current steady state (during peptide application) and returned in the GΩ range (and the current returned to about the zero level) within 20 s after peptide removal from the external perfusion solution. The current activation and deactivation time constants were 10 s and 0.8 s, respectively; maximal current was 360 pA. Note the much smaller (*outward*) current amplitude recorded at +20 mV in respect to −20 mV, and the fast current activation (time constant: 0.6 s) upon hyperpolarising from 0 to −20 mV during peptide perfusion. *Inset*: the whole-cell current recording was smoothed (*lower trace*; see Methods) to accurately measure the delay of current activation (indicated by the *arrow*, 1.8 s) computed from the solution change (shown in the *upper trace*)

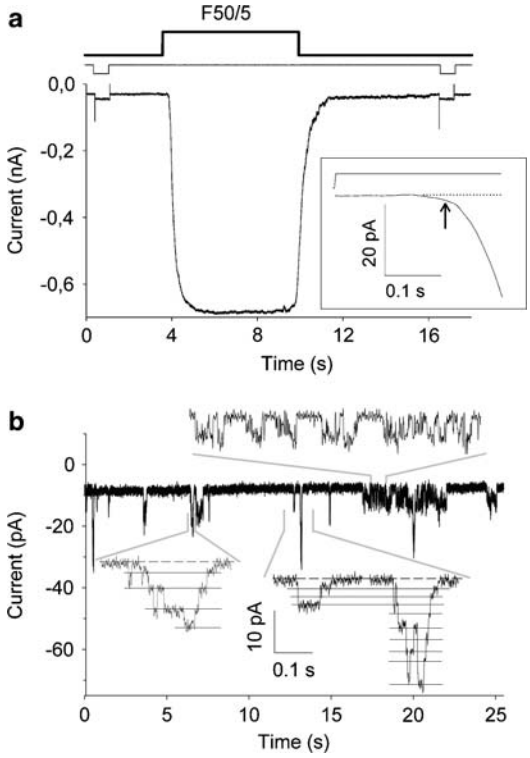

Fig. 4 Kinetics of OS membrane permeabilisation induced by 1 μM of synthetic alamethicin F50/5 and single channel activity recorded at 0.1 μM. **a** Traces show, from top to bottom, the timing of the peptide application and withdrawal, the timing of the two −10 mV voltage pulses (superimposed to $V_h = -20$ mV, used to measure R_m, that was about 1 GΩ before peptide application and 5 s after its removal), and the voltage-clamp, whole-cell current recording from the OS. The current activation and deactivation time constants were 0.21 s and 0.29 s, respectively; maximal current was 700 pA. *Inset*: the whole-cell current recording was smoothed (*lower trace*; see Methods) to accurately measure the delay of current activation (indicated by the *arrow*, 0.17 s) computed from the solution change (shown in the *upper trace*). **b** Single channel current recorded from an *OS* perfused with 0.1 μM of F50/5; to have clearly detectable single channel events V_h was −40 mV. In the typical recording shown, lasting 26.6 s, 1863 events were discerned, that could be grouped in the following four discrete levels: 2.2 pA, $n = 1564$; 2.8 pA, $n = 79$; 23.3 pA, $n = 218$; 4.0 pA, $n = 2$; n is the number of openings detected for each amplitude

of seconds to form functioning pores. The continuous peptide application produces more and more pores up to a steady number within a few seconds. The pores are rapidly lost, within about a couple of seconds, once the peptide is removed from the external solution. This is surprising, as the pore formed by alamethicin is expected be a relatively stable structure in the lipid phase, that should not disassemble that quickly once ceasing the continuous supply of peptide.

As expected (Eisenberg et al. 1973; reviewed in Toniolo et al. 2001), if alamethicin was applied at $V_h = +20$ mV, a small outward current (or no current at all) was recorded (Fig. 3). This finding indicates that alamethicin, applied to a membrane face, preferentially forms pores if the other membrane face is negatively charged. Moreover, hyperpolarisation from 0 to −20 mV during continuous perfusion with native alamethicin produced a current activation ~tenfold faster (0.72 ± 0.13 s, $n = 3$) than the one recorded by applying the peptide while the OS was hyperpolarised. This indicates that the pore can be pre-formed at 0 mV.

The soundness of this technique was further explored by using the synthetic alamethicin F50/5 (whose primary structure is reported in Methods), that circumvented the problems arising from unknown peptide mixture. This peptide exhibited a much higher capability to quickly insert in the membrane and form pores than native alamethicin mixture. Indeed, application of 1 μM concentration of alamethicin F50/5 activated a current with a delay 9-fold shorter (average: 210 ± 30 ms, $n = 10$; Fig. 4b) than that of alamethicin mixture. This current increased exponentially to a steady state, with an activation time constant and a maximal current that were ~30-fold faster (260 ± 20 ms, $n = 10$) and ~2-fold larger (703 ± 30 pA, $n = 10$) than those of the native alamethicin mixture (Fig. 4a). As it was found for the latter peptide, the permeabilisation induced by alamethicin F50/5 was fully reversible once it was removed from the external solution. The current returned to the zero level, without any delay with respect to the peptide removal time, with an exponential waveform having a deactivation time constant of 310 ± 20 ms ($n = 10$); R_m eventually recovered its previous (high) value (Fig. 4a) within 5 s following peptide removal. The above results show that even minor variations of the peptide sequence produces strong changes in the biophysical properties of the pore formed by the peptide in a natural membrane. This indicates that the peptaibol sequences could represent a potential leads for the development of bioactive peptides, and/or serve as targets for the development of therapeutic compounds.

Similarly to the native alamethicin, the F50/5 yielded very small outward currents when the OS was depolarised. For both peptides, maximal current amplitude and activation and deactivation time constants recorded in symmetric Na^+ were indistinguishable from the ones shown above (recorded in symmetric K^+), proving the poor cation selectivity of the channels formed by these peptides.

Clear single-channel events were recorded at low peptide concentrations (<250 nM), but several single channel current amplitudes were detected, being not a simple multiple of a fixed size. In Fig. 4b is shown a typical recording lasting ~27 s, where ~2000 events were discernible that could be grouped in 4 discrete levels of amplitude of ~2.2, ~2.8, ~3.3 and ~4.0 pA ($V_h = -40$ mV). Current bursts like that shown in the enlargements of Fig. 4b occurred at irregular intervals, making it difficult to investigate interval duration systematically and measure key parameters as the open probability, and the mean open and closed time of the channel levels. Therefore, just an estimate of the open

probability for all levels could be given, that was ~0.16 for the recording shown.

The range of single channel amplitudes could originate by the different number of helices constituting a single channel, that could vary with voltage, the peptide concentration and the duration of peptide application. Nevertheless, the fact that the current fell from several hundreds of pA to the single channel level following a four-fold reduction of peptide concentration, and that the peptide-elicited current fell to 0 within a few hundred of ms following peptide removal from the external solution, indicate that the pore formation and disaggregation are very fast and cooperative events.

Another peptaibol tested was a synthetic analog of the natural peptide trichogin GA IV, extracted from the soil fungus *Trichoderma longibrachiatum*, having the sequence reported in the Methods. No current was recorded upon perfusing this peptaibol on the OS with concentrations up to 6 μM and for V_h ranging from −60 to +60 mV (data not shown), while this peptide was able to form pores in artificial membranes (Mazzuca et al. 2005) at a 0.5 μM concentration. This shows once more the necessity to investigate the pore formation in natural membranes in order to develop peptides with biotherapeutic applications.

Acknowledgments Many thanks to Prof. Claudio Toniolo and Dr. Chiara Baldini for kindly providing alamethicin F50/5 and trichogin GA IV, and to Emanuela Correggioli, Martina Infanti, and Alberto Milani for invaluable help in the experiments and data analysis. This work was supported by grants from the Ministero per l'Università e la Ricerca Scientifica e Tecnologica (MURST), Roma, from CNISM "progetti innesco 2006" (project MRP), and from the "Comitato dei sostenitori dell'Università di Ferrara" (Project "Trasporto di carica fotoindotto in materiali funzionali").

References

Auvin-Guette C, Rebufatt S, Prigent Y, Bodo B (1992) Trichogin A IV, an 11-residue lipopeptaibol from Trichoderma longibrachiatum. J Am Chem Soc 114:2170–2174

Bockmann RA, Hac A, Heimburg T, Grubmuller H (2003) Effect of sodium chloride on a lipid bilayer. Biophys J 85(3):1647–1655

Boheim G (1974) Statistical analysis of alamethicin in a black lipid membrane. J Membr Biol 19:277–303

Carrasco L (1995) Modification of membrane permeability induced by animal viruses. Adv Virus Res 45:61–112

Chen HM, Clayton AH, Wang W, Sawyer WH (2001) Kinetics of membrane lysis by custom lytic peptides and peptide orientations in membrane. Eur J Biochem 268(6):1659–1669

Duclohier H (2002) How do channel- and pore-forming helical peptides interact with lipid membranes and how does this account for their antimicrobial activity? Mini Rev Med Chem 2(4):331–342

Eisenberg M, Hall JE, Mead CA (1973) The nature of the voltage-dependent conductance induced by alamethicin in black lipid membranes. J Membr Biol 14(2):143–176

Gonzales ME, Carrasco L (2003) Viroporins. FEBS Lett 552(1):28–34

Heuck AP, Johnson AE (2002) Pore-forming protein structure analysis in membranes using multiple independent fluorescence techniques. Cell Biochem Biophys 36(1):89–101

Hille B (2001) Ionic channels of excitable membranes. Sinauer, Third edition

Killian JA, Nyholm TK (2006) Peptides in lipid bilayers: the power of simple models. Curr Opin Struct Biol 16(4):473–479

Mazzuca C, Stella L, Venanzi M, Formaggio F, Toniolo C, Pispisa B (2005) Mechanism of membrane activity of the antibiotic trichogin GA IV: a two-state transition controlled by peptide concentration. Biophys J 88(5):3411–3421

Moriondo A, Rispoli G (2003) A step-by-step model of phototransduction cascade shows that CA2+ regulation of guanylate cyclase accounts only for short-term changes of photoresponse. Photochem Photobiol Sci 2(12):1292–1298

Oh D, Shin SY, Lee S, Kang JH, Kim SD, Ryu PD, Hahm KS, Kim Y (2000) Role of the hinge region and the tryptophan residue in the synthetic antimicrobial peptides, cecropin A(1–8)-magainin 2(1–12) and its analogues, on their antibiotic activities and structures. Biochem 39(39):11855–11864

Peggion C, Formaggio F, Crisma M, Epand RF, Epand RM, Toniolo C (2003) Trichogin: a paradigm for lipopeptaibols. J Pept Sci 9:679–689

Peggion C, Coin I, Toniolo C (2004) Total synthesis in solution of alamethicin F50/5 by an easily tunable segment condensation approach. Biopolymers (Pept Sci) 76:485–493

Rispoli G, Sather WA, Detwiler PB (1993) Visual transduction in dialyzed detached rod outer segments from lizard retina. J Physiol 465:513–537

Rispoli G, Navangione A, Vellani V (1995) Transport of K+ by Na(+)-Ca2+, K+ exchanger in isolated rods of lizard retina. Biophys J 69:74–83

Rispoli G (1998) Calcium regulation of phototransduction in vertebrate rod outer segments. J Photochem Photobiol B 44(1):1–20

Saint N, Cadiou H, Bessin Y, Molle G (2002) Antibacterial peptide pleurocidin forms ion channels in planar lipid bilayers. Biochim Biophys Acta 1564(2):359–364

Toniolo C, Crisma M, Formaggio F, Peggion C, Epand RF, Epand RM (2001) Lipopeptaibols, a novel family of membrane active, antimicrobial peptides. Cell Mol Life Sci 58:1179–1188

Wallace DP, Tomich JM, Eppler JW, Iwamoto T, Grantham JJ, Sullivan LP (2000) A synthetic channel-forming peptide induces Cl(-) secretion: modulation by Ca(2+)-dependent K(+) channels. Biochim Biophys Acta 1464(1):69–82